NASA TECHNICAL NOTE

NASA TN D-5677

C. 1

NASA TN D-5677

A POLYNOMIAL METHOD FOR DETERMINING LOCAL EMISSION INTENSITY BY ABEL INVERSION

by Chul Park and Dan Moore

Ames Research Center
Moffett Field, Calif.

NATIONAL AERONAUTICS AND SPACE ADMINISTRATION • WASHINGTON, D. C. • FEBRUARY 1970

1. Report No. NASA TN D-5677	2. Government Accession No.	3. Recipient's Catalog No.
4. Title and Subtitle A POLYNOMIAL METHOD FOR DETERMINING LOCAL EMISSION INTENSITY BY ABEL INVERSION		5. Report Date February 1970 6. Performing Organization Code
7. Author(s) Chul Park and Dan Moore		8. Performing Organization Report No. A-3444
9. Performing Organization Name and Address NASA Ames Research Center Moffett Field, Calif. 94035		10. Work Unit No. 192-02-08-01-00-21 11. Contract or Grant No.
12. Sponsoring Agency Name and Address National Aeronautics and Space Administration Washington, D. C. 20546		13. Type of Report and Period Covered Technical Note 14. Sponsoring Agency Code

15. Supplementary Notes

16. Abstract

The Abel inversion is applied to the transformation of the measured line-of-sight integrated radiation intensity from an axially symmetric plasma light source into local emission intensity. Consideration of the physical features of the plasma light source shows that the most appropriate approximation of the radial variation of emission is an even-power polynomial. Thus, the measured integrated intensity is represented by a linear combination of Abel transforms of even powers. The formula is precise near the axis of symmetry even when the integrated intensity is known at only two or three lateral positions. The formula becomes inaccurate at large radial distances and is suitable mainly when the emission intensity decreases monotonically toward the boundary.

17. Key Words Suggested by Author(s) Abel transform (or function) Plasma diagnostics Optical measurement	18. Distribution Statement Unclassified - Unlimited

19. Security Classif. (of this report)	20. Security Classif. (of this page)	21. No. of Pages	22. Price*
Unclassified	Unclassified	18	$3.00

*For sale by the Clearinghouse for Federal Scientific and Technical Information
Springfield, Virginia 22151

A POLYNOMIAL METHOD FOR DETERMINING LOCAL EMISSION INTENSITY BY ABEL INVERSION

By Chul Park and Dan Moore

Ames Research Center

SUMMARY

The Abel inversion is applied to the transformation of the measured line-of-sight integrated radiation intensity from an axially symmetric plasma light source into local emission intensity. Consideration of the physical features of the plasma light source shows that the most appropriate approximation of the radial variation of emission is an even-power polynomial. Thus, the measured integrated intensity is represented by a linear combination of Abel transforms of even powers. The formula is precise near the axis of symmetry even when the integrated intensity is known at only two or three lateral positions. The formula becomes inaccurate at large radial distances and is suitable mainly when the emission intensity decreases monotonically toward the boundary.

INTRODUCTION

The intensity of radiation energy observed from an optically thin plasma is an integrated sum of the intensity of emission per unit volume along the viewing line. When the plasma is axially symmetric, the radiative emission per unit volume, defined here as emission intensity (or simply emission), can be calculated from the observed integrated radiation intensity (or integrated intensity) by solving Abel's integral equation through inversion (ref. 1).

In the process of Abel inversion, it is necessary to differentiate the experimentally obtained integrated intensity distribution with respect to the distance along which it varies. Because the numerical differentiation magnifies the errors in the original data, most methods of Abel inversion result in a large magnification of the experimental error, which is proportional to the total number of points taken and is severest at the axis of symmetry. Typically, there is a tenfold magnification of error when the intensities are taken over 20 equally spaced intervals.

To reduce the effects of experimental error, one ordinarily smooths the data by fitting (in a least-squares sense) a polynomial curve through the data points. The corresponding curve points are then used as data points before applying the Abel inversion to determine the emission. The number of terms in the smoothing polynomial can be increased to reduce the sum of squares of the deviations of the observed data from the theoretical curve. However, high-order polynomials will oscillate, and the variation in slopes will

increase. Thus, one is compelled to smooth the data with a low-order polynomial. A data fit with a low-degree polynomial, however, results in an analytical error, that is, the error caused by failing to approximate a true variation by a simple analytical expression. Therefore, in current Abel inversion methods, a certain amount of error is introduced regardless of the number of points taken to represent the measured distribution of integrated intensity.

The purpose of the present work is to derive a new method for Abel inversion, applicable in certain cases, that will minimize the effects of experimental error in determining emission intensity on and near the axis of symmetry. Plasma emission intensity is assumed to vary such that it can be expressed by a polynomial in even powers of the radial distance. The experimental data, the integrated intensities, are fitted with a simple function that, after Abel inversion, produces a polynomial of even powers. This method is applied to two sets of typical experimental data. The proposed method is shown to be accurate near the axis of symmetry at least to the same degree as existing methods, even when only two or three data points are taken.

DERIVATION OF METHOD

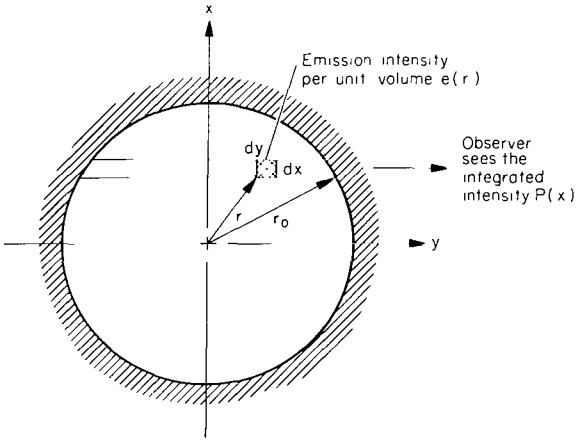

Figure 1.- Cross section of axially symmetric, optically thin radiation source.

Figure 1 is a cross section of the axisymmetric plasma under consideration. When the plasma is optically thin, the radiation intensity measured by an observer is an integrated sum of volumetric emission that varies with lateral displacement x of the viewing line. It has been shown (ref. 1) that integrated intensity $P(x)$ is an Abel transform of emission intensity $e(r)$; that is,

$$P(x) = 2\int_{x}^{r_o} \frac{e(r)\,r\,dr}{\sqrt{r^2 - x^2}} \qquad (1)$$

where r_o is the radius of the plasma boundary. The emission function $e(r)$ can be determined (ref. 1) from equation (1) through Abel's inversion to obtain

$$e(r) = -\frac{1}{\pi}\int_{r}^{r_o} \frac{(dP/dx)\,dx}{\sqrt{x^2 - r^2}} \qquad (2)$$

In most laboratory plasmas, the following features exist:

1. At the origin, that is, on the axis of symmetry ($r = 0$), the emission intensity is finite.

2. The derivative de/dr approaches zero as r approaches zero.

3. At the boundary ($r = r_o$), the derivative $(de/dr)_{r_o}$ is finite.

Analytical error can be minimized by fitting the most appropriate function to the observed integrated intensity $P(x)$. Table 1 lists four classes of functions that involve polynomials and their Abel inversions. As shown in table 1, if an even-power function represents the integrated intensity, the slope of emission function at the boundary is infinite. This feature is in conflict with the physical nature of plasma, (3) above, and so the method becomes inaccurate near the boundary. The odd-power functions have singularities not only at the boundary but also at the origin. For example, the linear function $P(x) = x$ implies infinite emission at the origin. For other odd-power functions, there is a term of the form $r^{2n} \ln r$ in the expressions for the emission, which has an infinite curvature at the origin; that is, the function $e(r)$ exhibits a finite slope in the region near (but not at) the origin, contrary to (2) above.

Because there is no singularity in the emission function in the range $0 \le r \le r_o$, the emission can always be approximated by a series in powers of r. Table 1 shows the functions $P(x)$ corresponding to the power functions of r. For the emission function to be an odd-power function of r, the integrated intensity must have a logarithmic variation near the origin. Because the logarithmic term is undesirable, the preferred form of emission is an even-power polynomial

$$e(r) = \sum_{i=0}^{m} b_i r^{2i} \tag{3}$$

in which m determines the last term of the series. It can be shown from table 1 that the corresponding function for the integrated intensity is

$$P(x) = \sqrt{r_o^2 - x^2} \sum_{i=0}^{m} a_i x^{2i} \tag{4}$$

Thus, when the experimentally determined integrated-intensity distribution is represented with a function of the form equation (4), a high degree of accuracy is attained near the origin $r = 0$.

The coefficients a_i and b_i in equations (3) and (4) are related through Abel's integral equation (1) (or eq. (2)). This relationship between the a_i and b_i is derived by substituting equation (3) into equation (1), as described in appendix A. For values of m up to 5, explicit formulas for determining b_i from given values of a_i are presented in table 2.

TABLE 1.- ABEL TRANSFORMS OF FUNCTIONS INVOLVING POLYNOMIALS

$P(x)$	$e(r) = -\frac{1}{\pi}\int_r^{r_o} \frac{P'(x)\,dx}{\sqrt{x^2 - r^2}}$	$\left(\frac{de}{dr}\right)_o$	$\left(\frac{d^2e}{dr^2}\right)_o$	$\left(\frac{de}{dr}\right)_{r_o}$
1	0	0	0	∞
x^2	$-\frac{2}{\pi}\sqrt{r_o^2 - r^2}$	0	0	∞
x^4	$-\frac{4}{3\pi}(r_o^2 + 2r^2)\sqrt{r_o^2 - r^2}$	0	0	∞
. . .	. . .	. . .	. . .	. . .
x^{2n}	$\sqrt{r_o^2 - r^2}\ \text{poly}(r^2)^a$	0	0	∞
x	$-\frac{1}{\pi}\ln\frac{r_o + \sqrt{r_o^2 - r^2}}{r}$	∞	∞	Finite
x^3	$-\frac{3}{\pi}\left(\frac{r_o}{2}\sqrt{r_o^2 - r^2} + \frac{r^2}{2}\ln\frac{r_o + \sqrt{r_o^2 - r^2}}{r}\right)$	$0(r \ln r)$	∞	∞
. . .	. . .	. . .	. . .	. . .
x^{2n+1}	$\ln\frac{r_o + \sqrt{r_o^2 - r^2}}{r}\ \text{poly}(r^2) + \sqrt{r_o^2 - r^2}\ \text{poly}(r^2)$	$0(r^n \ln r)$	0	∞
$2\sqrt{r_o^2 - x^2}$	1	0	0	0
$\frac{2}{3}(r_o^2 + 2x^2)\sqrt{r_o^2 - x^2}$	r^2	0	0	Finite
$\frac{2}{15}(3r_o^4 + 4x^2r_o^2 + 8x^4)\sqrt{r_o^2 - x^2}$	r^4	0	0	Finite
. . .	. . .	. . .	. . .	. . .
$\sqrt{r_o^2 - x^2}\ \text{poly}(x^2)^b$	r^{2n}	0	0	Finite
$r_o\sqrt{r_o^2 - x^2} + x^2\ln\frac{r_o + \sqrt{r_o^2 - x^2}}{x}$	r	0	0	0
$\frac{r_o}{2}\left(r_o^2 + \frac{3}{2}x^2\right)\sqrt{r_o^2 - x^2} + \frac{3}{4}x^4\ln\frac{r_o + \sqrt{r_o^2 - x^2}}{x}$	r^3	0	0	Finite
. . .	. . .	. . .	. . .	. . .
$\sqrt{r_o^2 - x^2}\ \text{poly}(x^2) + \ln\frac{r_o + \sqrt{r_o^2 - x^2}}{x}\ \text{poly}(x^2)$	r^{2n+1}	0	0	Finite

[a] $\text{Poly}(r^2)$ represents an even-power polynomial in r.

[b] $\text{Poly}(x^2)$ represents an even-power polynomial in x.

TABLE 2.- COEFFICIENTS b_n IN $e(r) = \sum_{n=0}^{m} b_n r^{2n}$ AS DETERMINED FROM THE COEFFICIENTS a_n IN $P(x) = \sqrt{r_o^2 - x^2} \sum_{n=0}^{m} a_n x^{2n}$ FOR ARBITRARY m

2 Terms
$b_o = a_o - 0.5a_1 r_o^2$
$b_1 = 1.5a_1$
3 Terms
$b_o = a_o - 0.5a_1 r_o^2 - 0.125a_2 r_o^4$
$b_1 = 1.5a_1 - 0.75a_2 r_o^2$
$b_2 = 2.125a_2$
4 Terms
$b_o = a_o - 0.5a_1 r_o^2 - 0.125a_2 r_o^4 - 0.0625a_3 r_o^6$
$b_1 = 1.5a_1 - 0.75a_2 r_o^2 - 0.1875a_3 r_o^4$
$b_2 = 2.125a_2 - 0.9375a_3 r_o^2$
$b_3 = 2.1875a_3$
5 Terms
$b_o = a_o - 0.5a_1 r_o^2 - 0.125a_2 r_o^4 - 0.0625a_3 r_o^6 - 0.03125a_4 r_o^8$
$b_1 = 1.5a_1 - 0.75a_2 r_o^2 - 0.1875a_3 r_o^4 - 0.09375a_4 r_o^6$
$b_2 = 2.125a_2 - 0.9375a_3 r_o^2 - 0.23437a_4 r_o^4$
$b_3 = 2.1875a_3 - 1.09375a_4 r_o^2$
$b_4 = 2.4609a_4$

DETERMINATION OF THE COEFFICIENTS a_i

When the integrated intensity $P(x_j)$ is known at $M + 1$ equally spaced points $x_0 = 0$, $x_1 = r_0/M$, $x_2 = 2r_0/M$, . . . , $x_j = jr_0/M$, . . . , where M is the number of zone divisions, the coefficients a_i of equation (4) can be determined from the set of $M + 1$ linear equations

$$\frac{P(x_j)}{r_0\sqrt{1 - (j/M)^2}} = \sum_{i=0}^{M} a_i\left(\frac{jr_0}{M}\right)^{2i}, \qquad j = 0, 1, 2, \ldots, M \tag{5}$$

However, it must be noted that when $j = M$, the left side of equation (5) is undefined. Physically, this difficulty is caused by the fact that both the light-emitting volume and the integrated intensity vanish at $x = r_0$. By taking the limit $x \to r_0$ in equation (2), there follows

$$e(r_0) = \frac{1}{2}\lim_{x \to r_0} \frac{P(x)}{\sqrt{r_0^2 - x^2}} \tag{6}$$

Because both the numerator and the denominator in the right side of equation (6) vanish, it is impossible to determine $e(r_0)$ experimentally without making a suitable assumption on the behavior of $P(x)$ near r_0. Two methods were developed to resolve this difficulty to satisfy two types of edge conditions.

Method 1

In the first method, the $M + 1$ equation is deleted so that only M linear equations remain to be solved:

$$\frac{P(x_j)}{r_0\sqrt{1 - (j/M)^2}} = \sum_{i=0}^{M-1} a_i\left(\frac{jr_0}{M}\right)^{2i}, \qquad j = 0, 1, 2, \ldots, M - 1 \tag{7}$$

This gives rise to an M term approximation for the emission function. When the last equation in (5) is deleted, the emission function is left to take an arbitrary finite value at the boundary as dictated by the function values at all other points. The $e(r_0)$ value given by this method may not be correct, but it is valid as long as $e(r)$ obeys the polynomial variation law of (3) near r_0. This method should be used if the variation of $e(r)$ with r is mild and if $e(r_0)$ is known to be finite, as in the case of the radiating shock layer around the nose of a body of revolution moving at high speed. The solutions for a_i employing this method are presented in table 3.

TABLE 3.- COEFFICIENTS b_i IN $e(r) = \sum_{i=0}^{m} b_i r^{2i}$ AS DETERMINED FROM $P(x_j)$, $(x_j = jr_o/M,\ j = 0, 1, \ldots, M)$; METHOD 1 ($m = M-1, e(r_o) \neq 0$ ASSUMED)

2 Zones, 2 Terms (M = 2, m = 1)
$b_o = [1.5P(o) - 1.1547P(r_o/2)]/r_o$
$b_1 = [-3P(o) + 3.4641P(r_o/2)]/r_o^3$
3 Zones, 3 Terms (M = 3, m = 2)
$b_o = [2.0469P(o) - 1.3921P(r_o/3) - 0.3144P(2r_o/3)]/r_o$
$b_1 = [-16.0313P(o) + 20.2851P(r_o/3) - 4.1507P(2r_o/3)]/r_o^3$
$b_2 = [18.9844P(o) - 26.8480P(r_o/3) + 8.4901P(2r_o/3)]/r_o^5$
4 Zones, 4 Terms (M = 4, m = 3)
$b_o = [3.2778P(o) - 2.7541P(r_o/4) + 0.0770P(r_o/2) - 0.2688P(3r_o/4)]/r_o$
$b_1 = [-43.0000P(o) + 55.7710P(r_o/4) - 13.1636P(r_o/2) + 0.6047P(3r_o/4)]/r_o^3$
$b_2 = [146.6667P(o) - 216.8871P(r_o/4) + 83.1384P(r_o/2) - 13.1028P(3r_o/4)]/r_o^5$
$b_3 = [-124.4444P(o) + 192.7885P(r_o/4) - 86.2176P(r_o/2) + 18.8142P(3r_o/4)]/r_o^7$
5 Zones, 5 Terms (M = 5, m = 4)
$b_o = [3.0694P(o) - 1.6997P(r_o/5) - 0.9633P(2r_o/5) + 0.1274P(3r_o/5) - 0.2052P(4r_o/5)]/r_o$
$b_1 = [-93.2719P(o) + 124.2254P(r_o/5) - 34.1480P(2r_o/5) + 4.1847P(3r_o/5) - 0.8236P(4r_o/5)]/r_o^3$
$b_2 = [579.7068P(o) - 877.7189P(r_o/5) + 369.2683P(2r_o/5) - 78.0015P(3r_o/5) + 7.0663P(4r_o/5)]/r_o^5$
$b_3 = [-1260.9694P(o) + 2010.7037P(r_o/5) - 997.0724P(2r_o/5) + 283.9830P(3r_o/5) - 37.4405P(4r_o/5)]/r_o^7$
$b_4 = [834.4651P(o) - 1362.6757P(r_o/5) + 728.3808P(2r_o/5) - 238.4186P(3r_o/5) + 39.7364P(4r_o/5)]/r_o^9$

TABLE 4.- COEFFICIENTS b_i IN $e(r) = \sum_{i=0}^{m} b_i r^{2i}$ AS DETERMINED FROM $P(x_j)$, $(x_j = jr_o/M,\ j = 0, 1, \ldots, M)$; METHOD 2 (m = M, $e(r_o) = 0$ ASSUMED)

2 Zones, 3 Terms (M = 2, m = 2)
$b_o = [1.5P(o) - 1.1570P(r_o/2)]/r_o$
$b_1 = [-5.25P(o) + 6.9282P(r_o/2)]/r_o^3$
$b_2 = [3.75P(o) - 5.7735P(r_o/2)]/r_o^5$
3 Zones, 4 Terms (M = 3, m = 3)
$b_o = [2.2266P(o) - 1.6780P(r_o/3) - 0.1698P(2r_o/3)]/r_o$
$b_1 = [-19.1016P(o) + 25.1700P(r_o/3) - 6.6223P(2r_o/3)]/r_o^3$
$b_2 = [39.0234P(o) - 58.7300P(r_o/3) + 24.6212P(2r_o/3)]/r_o^5$
$b_3 = [-22.1484P(o) + 35.2379P(r_o/3) - 17.8291P(2r_o/3)]/r_o^7$
4 Zones, 5 Terms (M = 4, m = 4)
$b_o = [3.0556P(o) - 2.3870P(r_o/4) - 0.1285P(r_o/2) - 0.1920P(3r_o/4)]/r_o$
$b_1 = [-47.9167P(o) + 63.8956P(r_o/4) - 17.7054P(r_o/2) + 2.3038P(3r_o/4)]/r_o^3$
$b_2 = [200.4167P(o) - 305.7075P(r_o/4) + 132.7906P(r_o/2) - 31.6700P(3r_o/4)]/r_o^5$
$b_3 = [-295.5556P(o) + 475.5450P(r_o/4) - 244.2833P(r_o/2) + 77.9447P(3r_o/4)]/r_o^7$
$b_4 = [140.0000P(o) - 231.3962P(r_o/4) + 129.3265P(r_o/2) - 48.3795P(3r_o/4)]/r_o^9$
5 Zones, 6 Terms (M = 5, m = 5)
$b_o = [3.7293P(o) - 2.8221P(r_o/5) - 0.2776P(2r_o/5) - 0.1672P(3r_o/5) - 0.1180P(4r_o/5)]/r_o$
$b_1 = [-97.8760P(o) + 132.0571P(r_o/5) - 38.9323P(2r_o/5) + 6.2401P(3r_o/5) - 1.4326P(4r_o/5)]/r_o^3$
$b_2 = [696.2967P(o) - 1076.0422P(r_o/5) + 490.4206P(2r_o/5) - 130.0505P(3r_o/5) + 22.4882P(4r_o/5)]/r_o^5$
$b_3 = [-1937.2940P(o) + 3161.1553P(r_o/5) - 1699.8635P(2r_o/5) + 585.9137P(3r_o/5) - 126.9015P(4r_o/5)]/r_o^7$
$b_4 = [2253.0556P(o) - 3775.7473P(r_o/5) + 2202.4849P(2r_o/5) - 871.7180P(3r_o/5) + 227.3807P(4r_o/5)]/r_o^9$
$b_5 = [-917.9116P(o) + 1561.3993P(r_o/5) - 953.8320P(2r_o/5) + 409.7820P(3r_o/5) - 121.4169P(4r_o/5)]/r_o^{11}$

Method 2

In the second method, emission is assumed to be zero at the boundary. Thus the full set of $M + 1$ linear equations in equation (5) was solved with the condition

$$\frac{P(x_j)}{r_o \sqrt{1 - (j/M)^2}} = 0 , \qquad j = M \tag{8}$$

This method of solution provides an emission function of $M + 1$ terms and is valid only when the emission decreases at a finite rate to zero at the boundary (see eq. (6)). The results are presented in table 4.

Since two methods of solutions of equation (5) were employed, the upper limit in the summation in equation (5) will be designated by m, where $m = M$ or $m = M - 1$ depending on which method is used. Appendix B presents the method of computing the coefficients a_i, and hence b_i, from the given $P(x_j)$ for arbitrary values of m up to 5.

COMPARISON OF RESULTS

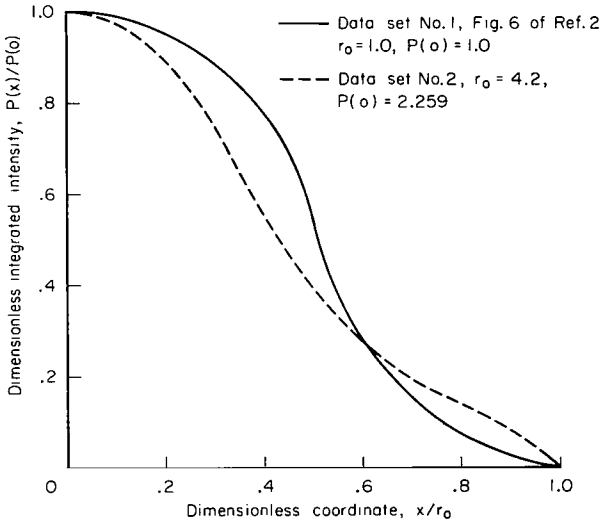

Figure 2.- Two sets of integrated intensity data used for testing the present method.

Formulas derived in the preceding sections are applied to the two sets of experimental data shown in figure 2. Data set no. 1 is taken from figure 6 of reference 2. Data set no. 2 was obtained by one of the present authors during an experiment with an arc-heated wind tunnel (ref. 3). The measured integrated intensity corresponding to data set no. 2 is the continuum emission at wavelengths near 4000 Å from ionized nitrogen flowing through a wind tunnel. As shown, both sets of data have been smoothed so that no error would be introduced or amplified because of experimental scatter. The comparison thus tests the capability of the present method to yield the same inversion as can be attained by existing inversion methods in the absence of experimental scatter. Except for the method of reference 2, which uses an analog computer, the existing methods use high-order (20- or 30-zone) formulas for greater accuracy. The present method limits the number of zones to 5; a larger number results in oscillations at larger values of r.

Data Set No. 1

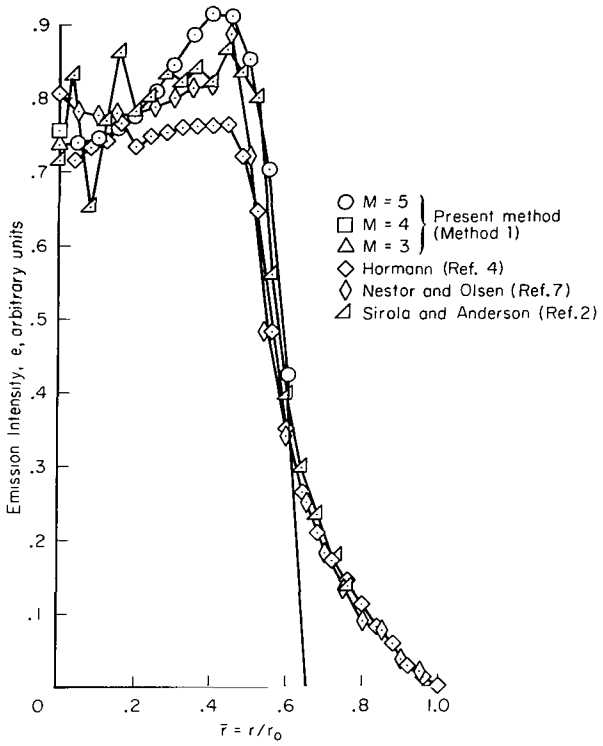

(a) Data set no. 1.

Figure 3.- Emission intensity obtained by inversion of test data in figure 2.

In figure 3(a), the present method of inversion is compared with other methods for the first set of data. A 5-zone inversion formula of method 1 (formula 4 of table 3) is chosen for this comparison. Corresponding results with 4-zone, 4-term and 3-zone, 3-term formulas also are shown for the origin r = 0. The results of inversions by Sirola and Anderson (ref. 2) and Hörmann (ref. 4) are reproduced from reference 2. (The method of Sirola and Anderson is based on the analysis of Pearce (ref. 5).) Bockasten's method (ref. 6) also was used; the result agreed closely (a 2-percent discrepancy) with that obtained by Nestor and Olsen (ref. 7).[1] Edels, Hearne, and Young (ref. 8) reproduced independently the results obtained by Nestor and Olsen and by Bockasten.

Figure 3 indicates that the methods of both Hörmann and Pearce (i.e., Sirola and Anderson) fail at the origin. Hörmann's method fails because of the necessity to evaluate the area under an undefined curve near the origin. Pearce's method breaks down because it assumes a step-function variation of integrated intensity that cannot describe the emission intensity near the origin. The method of Nagler (ref. 9) is similar to that of Pearce. The method of Dooley and McGregor (ref. 10) is similar to that of Hörmann and has the same mathematical difficulty caused by the singularity at the origin. In the case of the Hörmann inversion, and therefore Dooley and McGregor inversion, the error due to the singularity at the origin adds to the deduced value of emission over the entire range.

The methods of Nestor and Olsen and of Bockasten (or equivalently Edels et al.) result in definite values for the emission at the origin because the linear term is excluded in the integrated intensity (see table 1). However, in these methods, the cubic term x^3 is allowed as well as x^2, leading to infinite curvature at the origin (see table 1). As a result, the derived emission-intensity gradient is finite near the origin as shown, even though the gradient of integrated intensity should be zero at the origin. This contradicts the physical nature of the problem (feature (2) stated earlier).

[1]The profile inverted by the Nestor-Olsen method shown in figure 3(a) is different from the corresponding profile in reference 2. As implied in reference 2, the Nestor-Olsen profile was found to be in error.

Nevertheless, of the existing methods, these of Nestor and Olsen and of Bockasten appear the most accurate; Bockasten's is preferred because of its closer piecewise curve fit (parabolic vs. linear for Nestor and Olsen) to the integrated intensity.

The present method provides a well-defined finite emission value at the origin and a smooth parabolic change near the origin. The peak value of emission intensity calculated by the present method agrees closely with those obtained by the better of the existing methods. The present method fails, however, at large values of $\bar{r} \equiv r/r_o$, that is, $\bar{r} \gtrsim 0.6$ for the present test data, because:

1. The formula used here (method 1) leaves the emission arbitrary at the boundary.

2. Expansions of the form of equation (4) tend to oscillate as $r/r_o \to 1$.

Point (2) is a result of the emission-function peak at an intermediate point, around $\bar{r} = 0.5$, which decays rapidly as $\bar{r}$ increases toward unity. Thus, the present method is not suitable for calculating the emission at large radial distances when the slopes are changing rapidly (see fig. 2). At the origin, however, even a 3-zone formula of either method 1 or 2 gives a satisfactory result. As seen from figure 3, existing methods are satisfactory at large radial distances. It is possible to improve the present method for large $\bar{r}$, for example, by expanding in power series around r_o instead of the origin; however, no such attempt was made since most existing methods yield satisfactory results in this region.

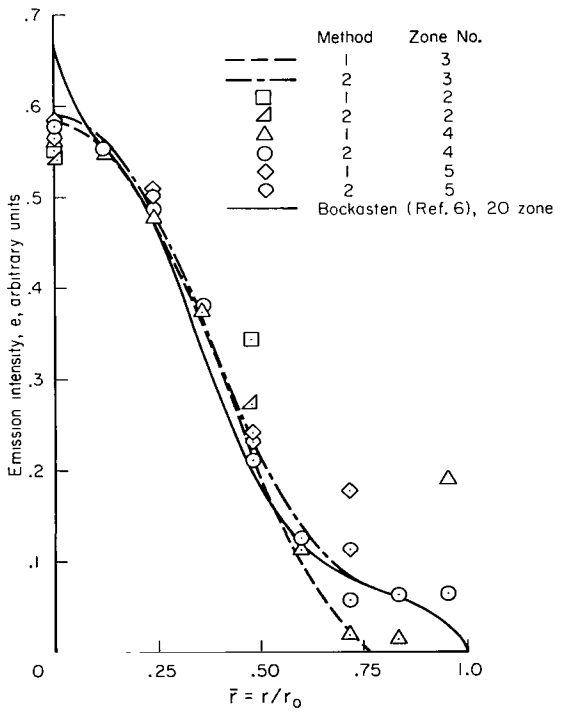

(b) Data set no. 2.

Figure 3.- Concluded.

Data Set No. 2

Figure 3(b) compares different formulas of methods 1 and 2 with that of Bockasten for the second set of data. To avoid congestion, results are shown for selected radii for 2-, 4-, and 5-zone cases. For the 2-zone cases, the emission values are shown only at the origin and approximate midradius $\bar{r} = 0.47$, because these are sufficient to define the curve.

The Bockasten inversion, like that of Nestor and Olsen (fig. 3(a)), yields a sharp peak in emission at the origin. For the reason noted earlier, the Bockasten value at the origin cannot be trusted. For the rest of the range, except near the plasma boundary, methods 1 and 2 formulas of order 3 and above yield results that agree closely with that of Bockasten. Generally, the

higher order formulas tend to oscillate near the boundary. The amplitude of the oscillations are greater for method 1 than for method 2, which assumes that emission vanishes at the boundary. In particular, the 3-zone formula of method 2 agrees closely with the Bockasten result over the entire radius range. This agreement may be fortuitous and cannot be expected as a rule. Because none of the existing methods is accurate at the origin, it is not possible to assess the absolute accuracy of the present method at the origin. Such accuracy is strongly suggested, however, by the consistency of results yielded by all the formulas of different order, and by the mathematical rigor of the present method. Even a 2-zone, 2-term formula gives a value accurate to within 5 percent at the origin.

The present method results in high accuracy for data set no. 2 because the emission variation with radius is well behaved (fig. 3(b)). That is, the emission decreases monotonically toward the boundary, and the change in the slope of decay is gradual over the entire radius range. Because such a variation can be approximated accurately by a polynomial, a high degree of accuracy can be expected.

DISCUSSION

The sensitivity of the inversion to the initial input error in integrated intensity is shown in table 5. The numbers in the table represent the ratio of the output error in emission at the radii indicated to the input error in integrated intensity. Thus, for example, if one uses the 4-zone, 5-term formula for data set no. 1, and if the integrated intensity at $r = 0.5r_o$ is misread by 1 percent, the emission suffers an error of 1.18 percent at that point. The 2-zone, 2-term, and 3-term calculation for data set no. 1 are not listed because the 2-term formulas are inappropriate.

As shown, the present method is much less sensitive to experimental error than the existing methods, at least in the range $0 < r < 0.5r_o$. Note that the amplification of initial error is small with the present method even though the coefficients in the expressions of b_i in tables 3 and 4 are large numbers, especially for large m. It is essential, however, that the values of $P(jr_o/M)$ be represented by a sufficiently large number of digits in the calculation of b_i for all i. A lower order formula magnifies the input error to a lesser degree. Again, this is expected: the greater the number of intervals at which a value of integrated intensity is read, the smaller the magnification of error by differentiation. For the same zone division, method 1 magnifies the error the least.

Any error in the determination of the overall radius of r_o is magnified by the inversion process. To determine the factor of magnification of such an error, one first changes r_o deliberately by an amount Δr_o so that the jth zone point is shifted by $(j/M)\Delta r_o$, and computing the emission function e on the basis of the values of P at the new zone points. This calculation is carried out for data set no. 2 for the present method and for the 10-zone Bockasten formula. Table 6 shows the results of the calculation. The figures

TABLE 5.- COMPARISON OF INVERSION METHODS FOR MAGNIFICATION[a] OF EXPERIMENTAL ERROR

	Data set no. 1		Data set no. 2	
	r = 0	r = $r_o/2$	r = 0	r = $r_o/2$
Bockasten (ref. 6)				
M = 20	18.8	1.88	14.2	3.08
Nestor and Olsen (ref. 7)				
M = 20	15.8	2.17	11.8	3.40
M = 50	39.5	5.43	29.5	8.50
Method 1				
m = 2	---	---	1.44	.20
m = 3	2.77	.61	1.90	.27
m = 4	3.47	.76	2.38	.33
m = 5	4.16	.91	2.85	.40
Method 2				
m = 2	---	---	1.42	.26
m = 3	3.11	.91	2.03	.37
m = 4	4.02	1.18	2.85	.52
m = 5	4.97	1.46	3.46	.63

[a]Ratio of the error in emission intensity e(r) to the error in the integrated intensity P(x).

TABLE 6.- COMPARISON OF PRESENT AND BOCKASTEN INVERSION METHODS FOR MAGNIFICATION OF ERROR IN r_o*

	M = 2	M = 3	M = 4	M = 5	M = 10
Method 1	1.14	1.51	1.67	1.72	---
Method 2	1.14	1.67	1.70	1.57	---
Bockasten	---	---	---	---	1.18

*Ratio of error in emission intensity at the origin caused by the error in r_o to the error in r_o, for data set no. 2.

in the table represent the magnification factor, that is, the ratio of the error in the resulting emission intensity at the origin $e(0)$ caused by the error in r_o to the error in r_o itself. The 10-zone (rather than 20-zone) Bockasten formula was used because it was difficult to read small changes in $P(x)$ caused by the shifting of x by $(j/M)\Delta r_o$. As indicated by table 6, the magnification of the error in r_o by the inversion remains the order of unity for both the present and Bockasten's methods.

In the present method, a truncation error exists in addition to the experiment-originated errors mentioned above. Because the basic polynomial representations, equations (3) and (4), truncate a Maclaurin infinite series at the mth term, there always exists an error of the same magnitude as the $m + 1$ term. The accuracy of the present method depends, among other things, on how accurately the functions e and P can be approximated by the forms of equations (3) and (4). The truncation error is small near the origin, but becomes large at large r, especially for large m, making the present method invalid at large r.

The curvature of emission variation with radius at the axis is given in the present method as

$$\frac{d^2e}{dr^2} = 2b_1$$

where b_1 is as listed in tables 3 and 4. The accuracy of the derived curvature will improve as the degree of the polynomial is increased provided that the input data are absolutely accurate. None of the existing methods, however, can satisfactorily resolve emission profile curvature on the axis of symmetry.

When the integrated intensity is not known at equally spaced points $x = jr_o/M$, the formulas of tables 3 and 4 cannot be used. The present method can still be applied, however, with a minor modification: The curve of the form of equation (4) must be fitted to the experimental data; then the coefficients b_i can be determined as in appendix A or table 2.

Method 2 should be used if the emission is known to vanish at the boundary and if the values near the boundary are desired. Otherwise, method 1 is preferable because it is insensitive to initial input error. The required number of zones depends on the type of variation of integrated intensity. If the integrated intensity varies such that the emission varies monotonically with radius, and if there are no more than two inflection points, as in figure 4, a 3-zone subdivision should be adequate. If there is no inflection point in integrated intensity, as when the boundary is a bow shock wave over a spherical body moving through the atmosphere at very high speeds, a 2-zone formula may be accurate enough. The order of zoning should be increased as the number of inflection points is increased, because otherwise the polynomial cannot properly describe the variation. If it is not known *a priori* how many inflection points the emission function has, the calculation should be repeated with various zonings. The required number of zones will have been reached when further increases fail to change the calculated emission values.

The present method can be used most advantageously in experiments to determine the conditions of plasma produced in facilities for aerothermodynamic testing. In most such experiments in wind tunnels or shock tubes, it is necessary only to know the condition of the plasma at and near the centerline, that is, the emission and curvature at the origin. Also, in many cases, the flows produced in such facilities have maximum emission on the axis of symmetry, which is favorable for the present method.

CONCLUSIONS

The method for Abel inversion described uses only a few measured values of integrated radiation intensity. The emission intensity is described by an even-power polynomial in the radial coordinate r, the coefficients of which are determined to best fit the measured intensity. The inversion is accurate near the axis of symmetry, and breaks down at large radial distances. It is also more accurate when emissivity decreases monotonically toward the boundary than otherwise. The magnification of error in the inversion is much smaller than that present in other methods.

Ames Research Center
National Aeronautics and Space Administration
Moffett Field, Calif., 94035, Oct. 2, 1969

APPENDIX A

DETERMINATION OF b_i FROM a_i

By differentiating equation (4), one obtains

$$\frac{dP}{dx} = \frac{1}{\sqrt{r_o^2 - x^2}} \sum_{k=0}^{m} x^{2k+1}\left[2(k+1)a_{k+1}r_o^2 - (2k+1)a_k\right] \tag{A1}$$

Then one evaluates the integral

$$Q_k \equiv \int_r^{r_o} \frac{x^{2k+1}\,dx}{\sqrt{(x^2 - r^2)(r_o^2 - x^2)}} = \frac{1}{2}\frac{\pi}{4^k} \sum_{\ell=0}^{k} \binom{2\ell}{\ell}\binom{2k-2\ell}{k-\ell} r^{2\ell} r_o^{2(k-\ell)} \tag{A2}$$

Substitution of equations (A1) and (A2) into equation (2) yields

$$e(r) = -\frac{1}{\pi} \sum_{k=0}^{m} \left[(2k+2)a_{k+1}r_o^2 - (2k+1)a_k\right]Q_k \tag{A3}$$

Equating the coefficients of corresponding powers of r in expressions (3) and (A3), we obtain the coefficients b_i

$$b_i = \sum_{k=i}^{m} \frac{1}{2}\frac{1}{4^k}\binom{2k-2i}{k-i} r_o^{2k-2i}\binom{2i}{i}\left[(2k+1)a_k - (2k-2)a_{k+1}r_o^2\right] \tag{A4}$$

In terms of the a_k, equation (A4) becomes

$$b_i = \sum_{k=i}^{m} \left[(2k+1)B_{k,i} - 2kB_{k-1,i}\right] r_o^{2k-2i} a_k \tag{A5}$$

where

$$B_{k,i} = \frac{1}{2}\frac{1}{4^k}\binom{2k-2i}{k-i}\binom{2i}{i} \quad \text{for} \quad k \geq i \tag{A6}$$

The explicit numerical form of equation (A5) is presented in table 2 for values of m up to 5.

APPENDIX B

DETERMINATION OF a_i AND b_i FROM $P(x_j)$ FOR EQUALLY SPACED x_j

In the solution of equation (5), the values for $P(x)$ are assumed known at equally spaced points x_j

$$x_j = \frac{j}{M} r_o , \qquad j = 0, 1, 2, \ldots , M$$

Then equation (5) can be written as

$$\frac{P(jr_o/M)}{r_o \sqrt{1 - (j/M)^2}} = \sum_{k=0}^{m} a_k \left(\frac{jr_o}{M}\right)^{2k} \tag{B1}$$

Letting Y be a vector with components y_j, X a matrix with components X_{jk}, and A a vector with components a_k, where

$$y_j = \frac{P(jr_o/M)}{r_o \sqrt{1 - (j/M)^2}} , \qquad X_{jk} = \left(\frac{jr_o}{M}\right)^{2k} , \qquad \text{and} \qquad X_{\infty} = 1$$

we have the matrix representation of equation (B1)

$$Y = XA$$

Now we can find a solution matrix X^{-1} so that the a_k can be given by

$$a_k = \sum_{j=0}^{m} X_{kj}^{-1} y_j \tag{B2}$$

Substitution of equation (B2) into (A5) yields

$$b_i = \sum_{k=i}^{m} \sum_{j=0}^{m} \left[(2k + 1)B_{k,i} - 2kB_{k-1,i}\right] r_o^{2k-2n} X_{kj}^{-1} y_j \tag{B3}$$

where $B_{k,i}$ is given in equation (A6). The numerical form of equation (B3) is presented in tables 3 and 4 for values of m up to 5.

REFERENCES

1. Griem, H. R.: Plasma Spectroscopy. McGraw-Hill Book Co., Inc., 1964, pp. 176-178.

2. Sirola, R. O.; and Anderson, T. P.: Abel Integral Inverter. Rev. Sci. Instr., vol. 38, no. 6, 1967, pp. 749-759.

3. Stine, Howard A.; Watson, Velvin R.; and Shepard, Charles E.: Effect of Axial Flow on the Behavior of the Wall-Constricted Arc. Presented at AGARD Specialists' Meeting on Arc Heaters and MHD Accelerators for Aerodynamic Purposes (Rhode-Saint-Genese), Sept. 21-23, 1964. See also Park, Chul; and Okuno, Arthur F.: Diagnosis of High-Density Highly Ionized Nitrogen Wind-Tunnel Flows. Proc. 2nd Intl. Cong. on Instrumentation in Aerosp. Simulation Facilities, Stanford University, Aug. 1966, pp. 26-1 to 26-10.

4. Hörmann, H.: Temperaturverteilung und Electronendichte in freibrennenden Lichtbogen. Z. Physik, vol. 97, 1935, pp. 539-560.

5. Pearce, Willard J.: Measurement of Temperature of Arc Plasmas. Conf. on Extremely High Temperatures, H. Fisher and L. C. Mansur (eds.), John Wiley and Sons, Inc., 1958, pp. 123-133.

6. Bockasten, K.: Transformation of Observed Projected Intensities Into Radial Distribution of the Emission of a Plasma. Tech. Note 3, Inst. of Physics, Uppsala University, Sweden, 1960.

7. Nestor, O. H.; and Olsen, H. N.: Numerical Methods for Reducing Line and Surface Probe Data. SIAM Review, vol. 2, no. 3, 1960, pp. 200-207.

8. Edels, H.; Hearne, K.; and Young, A.; Numerical Solutions of the Abel Integral Equation. J. Math. Phys., vol. 41, 1962, pp. 62-75.

9. Nagler, Robert G.: Application of Spectroscopic Temperature Measuring Methods to Definition of a Plasma Arc Flame. JPL Tech. Rep. 32-66, Jan. 1961.

10. Dooley, M. T.; and McGregor, W. K.: Calculation of the Radial Distribution of the Density Dependent Properties in an Axisymmetric Gas Stream. AEDC Tech. Note 60-216, May 1961.

NASA-Langley, 1970 — 25 A-3444

"The aeronautical and space activities of the United States shall be conducted so as to contribute . . . to the expansion of human knowledge of phenomena in the atmosphere and space. The Administration shall provide for the widest practicable and appropriate dissemination of information concerning its activities and the results thereof."

—NATIONAL AERONAUTICS AND SPACE ACT OF 1958

NASA SCIENTIFIC AND TECHNICAL PUBLICATIONS

TECHNICAL REPORTS: Scientific and technical information considered important, complete, and a lasting contribution to existing knowledge.

TECHNICAL NOTES: Information less broad in scope but nevertheless of importance as a contribution to existing knowledge.

TECHNICAL MEMORANDUMS: Information receiving limited distribution because of preliminary data, security classification, or other reasons.

CONTRACTOR REPORTS: Scientific and technical information generated under a NASA contract or grant and considered an important contribution to existing knowledge.

TECHNICAL TRANSLATIONS: Information published in a foreign language considered to merit NASA distribution in English.

SPECIAL PUBLICATIONS: Information derived from or of value to NASA activities. Publications include conference proceedings, monographs, data compilations, handbooks, sourcebooks, and special bibliographies.

TECHNOLOGY UTILIZATION PUBLICATIONS: Information on technology used by NASA that may be of particular interest in commercial and other non-aerospace applications. Publications include Tech Briefs, Technology Utilization Reports and Notes, and Technology Surveys.

Details on the availability of these publications may be obtained from:

SCIENTIFIC AND TECHNICAL INFORMATION DIVISION

NATIONAL AERONAUTICS AND SPACE ADMINISTRATION

Washington, D.C. 20546